Title: Adsorption and desorption of single stranded DNA from single walled carbon nanotubes

Authors: Cameron James Shearer, Ph.D; LePing Yu; Renzo Fenati; Alex Sibley; Jamie Scott Quinton; Christopher Thomas Gibson; Amanda Vera Ellis; Gunther Andersson; Joseph George Shapter

To be cited as: Chem. Asian J. 10.1002/asia.201700446

Link to VoR: https://doi.org/10.1002/asia.201700446

Adsorption and desorption of single stranded DNA from single walled carbon nanotubes

Cameron J. Shearer,[a*] LePing Yu,[a] Renzo Fenati,[a,b] Alex Sibley, [a] Jamie S. Quinton,[a] Christopher T. Gibson,[a] Amanda V. Ellis,[a,b] Gunther G. Andersson,[a] Joseph G. Shapter [a*]

[a]Flinders Centre for NanoScale Science and Technology, School of Chemical and Physical Science, Flinders University, Bedford Park, South Australia 5042, Australia

[b]Present Address: School of Chemical and Biomolecular Engineering, University of Melbourne, Parkville, Victoria 3010, Australia

*Cameron.shearer@flinders.edu.au; Joe.shapter@flinders.edu.au School of Chemical and Physical Sciences, Flinders University, Sturt Rd, Bedford Park, South Australia 5042

Supporting information for this article is available on the WWW under http://dx.doi.org/10.1002/asia.201xxxxxx.

The chemical affinity of single stranded DNA (ssDNA) to adsorb to the surface of single walled carbon nanotubes (SWCNTs) is used for SWCNT purification, separation and in bio-devices. Despite the popularity of research on SWCNT-ssDNA conjugates, very little work has been dedicated to study the removal of adsorbed ssDNA on SWCNTs. This paper reports a comprehensive study of biological, physical and chemical treatments for the removal of ssDNA from SWCNT-ssDNA suspensions. These include enzymatic cleavage, heat treatment under vacuum up to 400 ^{o}C, chemical treatments with high or low pH, oxidising conditions, and high ionic strength solvents. Complimentary characterisation techniques including fluorescence from a DNA intercalating dye (YO-PRO-1) and photoelectron spectroscopy are used to exhaustively study and compare the methods investigated. Enzyme treatment is found to remove the phosphate backbone only, leaving nucleosides adsorbed to SWCNTs. Heating in inert atmosphere is ineffective at removing ssDNA. Acid, base and oxidative treatment are found to be effective for the removal of ssDNA from SWCNTs. Where possible the mechanism of desorption is described and from the findings suggestions for 'best practise' are provided.

Introduction

Single-walled carbon nanotubes (SWCNTs) exhibit mechanical, electrical and optical properties that make them attractive in a range of fields including photovoltaics, nanoelectronics, catalysis, biodevices and energy storage.[1] The intrinsic properties of an individual SWCNT depends upon its chiral indices (*n*, *m*) which in turn dictate whether the SWCNT is metallic or semiconducting and the energy of its optical/electronic band gap.[2] Despite tremendous effort, no synthesis method has been developed to produce chirality pure SWCNTs.[3] To obtain chirality pure SWCNT samples, various post processing sorting methods have been evaluated in which purification is achieved by utilizing slight variations in wrapping of polymers, surfactants or single stranded DNA (ssDNA) onto SWCNT with different chirality to drive separation.[4] From these methods ssDNA assisted wrapping has achieved the largest library of isolated (*n*, *m*) species due partly to the vast variety of ssDNA oligomer sequences possible.[5] Furthermore, the efficacy of ssDNA based separation has recently been further refined to separate SWCNT enantiomers.[6]

ssDNA adsorbs onto SWCNTs via attractive π-π interactions between nucleotides and the aromatic SWCNT side walls.[4c] The strong interaction results in ssDNA remaining adsorbed to the SWCNT which can alter and reduce intrinsic properties. In the case of biosensors, remaining ssDNA is used as a probe or transducer but in many applications remaining ssDNA is an unwanted by-product of SWCNT purification. Few studies have looked into the desorption of ssDNA from SWCNTs and fewer have conclusively given evidence for its removal. Oxidative treatment at elevated temperature (250 – 300 ^{o}C) has been used for the preparation of nanoelectronics with indirect evidence of removal obtained from transistor performance and atomic force microscopy (AFM).[7] The addition of complementary ssDNA has also been used to remove adsorbed ssDNA due to a higher affinity to form double stranded DNA (dsDNA) than remain on the SWCNT substrate. This method requires the addition of excess complimentary ssDNA has been used for development of biosensors and nanoelectronics.[8] A third reported method to remove ssDNA is to add the common SWCNT dispersing agent sodium dodecylbenzenesulfonate (SDBS), which can replace ssDNA as evidenced by a UV-Vis absorbance shift, however when following this method the surfactant remains adsorbed.[9]

Methods inspired by biology have also been investigated for the removal of ssDNA. SWCNTs dispersed by RNA have been treated with the enzyme ribonuclease (RNase) to digest the RNA. The authors found the stable SWCNT suspension precipitated upon RNase treatment and they observed a reduction in amorphous carbon but did not further investigate the efficacy of RNase.[10] In the case of more stable DNA and ssDNA, SWCNTs have been reported to restrict the action of an endonuclease enzyme DNase 1.[11] In this report the authors prepared a complicated biosensor system in which a fluorescently labelled ssDNA sequence $(GT)_{30}$ was adsorbed onto SWCNTs with the SWCNTs acting to quench the fluorescence. To show DNase 1 was restricted by the SWCNT: the SWCNT-ssDNA-fluorescent probe was treated with DNase 1, with the expectation that the fluorescent probe would desorb and become fluorescent if DNase 1 digested the ssDNA but this was not observed suggesting the SWCNT restricted DNase 1.[11]

SWCNT-ssDNA conjugates are clearly an attractive material for a range of applications,[1b] however greater evidence is clearly required to monitor the removal of ssDNA. This paper investigates and thoroughly characterises ssDNA removal using exonuclease 1 (exo1), heat treatment, HCl, NaOH, H_2O_2 and $MgCl_2$.

Experimental Details

SWCNT-ssDNA conjugate synthesis

SWCNTs (CoMoCAT, SG65 grade, Sigma Aldrich) were dispersed into water (MilliQ) at a concentration of 4 mg/mL and bath sonicated for 20 min. Custom made oligonucleotide ssDNA $(GT)_{20}$ (GeneWorks, Australia) were dispersed into water at a concentration of 10 mg/mL. The SWCNT and ssDNA stock suspension were mixed with NaCl solution to a final concentration of 0.1M NaCl, 2 mg/mL ssDNA, 1 mg/mL SWCNT. The suspension was probe-sonicated in an ice bath at 4 W/mL for 120 min. SWCNTs that were not individualised by ssDNA wrapping were removed via centrifugation at 17000g with fixed temperature (20 ^{o}C) for 90 min. The supernatant of suspended SWCNTs was collected and used for further investigation.

ssDNA desorption from SWCNTs

To remove excess amounts of free ssDNA in solution not conjugated to the SWCNTs, 25 µL of SWCNT-ssDNA conjugate solution was added to 475 µL of MilliQ water. The diluted conjugate solution was then placed in a AMICON Ultra 0.5 30K (Millipore,USA) centrifuge filtration vial, according to the recommendations of the manufacturer. The conjugate solution was eluted with 1X Exonuclease 1 reaction buffer.

For the removal of the DNA using exonuclease 1, the SWCNT were suspended in 1X Exonuclease 1 reaction buffer 50 µL. Exonuclease 1 (2.5 units) was added and pipette mixed, then placed in a thermocycler for 16 hrs at 37 ˚C. Afterwards the SWCNT were centrifuged to form a pellet at the bottom of the tube and the supernatant was removed, the pellet was resuspended in MilliQ water. The SWCNT were then purified using AMICON Ultra 0.5 30K again and washed three times with MilliQ water and eluted with 0.1 NaCl solution.

Precipitation of the ssDNA on the SWCNT was performed by adding equal amounts of SWCNT and 1 M $MgCl_2$ was combined into a tube. Once the SWCNT were precipitated out of the solution the supernatant solution was removed and the SWCNT were centrifuged to form a pellet then washed three times with MilliQ water and suspended with 0.1 NaCl solution.

Heat treatment was conducted by in situ heating within an ultrahigh vacuum photoemission spectroscopy apparatus via electron impact (SH100, SPECS, Germany) upon the sample holder. During heating the potential of the impacting electrons was 1000 V and the filament current was manually adjusted to increase heating rate. The heating rate was approximately 20 ^{o}C/min and was limited by the outgassing rate from the filament and sample (filament current was reduced if pressure exceeded $3x10^{-8}$ mbar) with heating held at 400 ^{o}C for 110 min and XPS spectra collected at intervals during heating. The temperature was monitored by a thermocouple (Eurotherm 2208e) on the sample mount. The pressure throughout the experiment was $3x10^{-10}$ - $3x10^{-8}$ mbar.

Chemical treatments were 1 M HCl (diluted from 37%, Sigma-Aldrich, Australia), 1 M NaOH (TCI chemicals, Japan) and 50 mM H_2O_2 (diluted from 30 %, Adelab Scientific, Australia). The chemical reagent was prepared to concentrations twice that used in reaction. An equal volume of SWCNT-ssDNA suspension was mixed with an equal volume of chemical reagent and vortex mixed for 1 min. The reaction was then transferred to a water bath at 25 ^{o}C or 60 ^{o}C and left for 2 h. The reaction was stopped by either centrifuge filtering and washing with 0.1M NaCl three times or depositing the sample onto a glass slide, drying in air at 30 ^{o}C then gently washing the dried precipitate with water and drying with three repetitions of this process.

YOPRO1 fluorescent probe with SWCNT-ssDNA

YO-PRO®-1 Iodide (491/509) (YOPRO1, 1mM in dimethylsulfoxide (DMSO), ThermoFisher, Y3603, Australia) was diluted to a stock suspension of 100 µM in water. YOPRO1 was added to SWCNT following two procedures. Liquid phase mixing involved mixing 15 µL 100 µM YOPRO1 with 35 µL SWCNT suspension for a final YOPRO1 concentration of 30 µM. The suspension was vortex mixed for 1 min, allowed to react for 30 min before being centrifuge filtered and resuspended into 0.1 M NaCl.

The dry reaction was completed by dropping the YOPRO1 stock solution onto a glass slide containing a dried sample of SWCNT (before or after chemical treatment) and drying in the dark at 30 ^{o}C. Positive and negative control experiments were completed for each reaction sequence as detailed in results and discussion.

Characterisation of SWCNT-ssDNA conjugates

UV-Vis-nIR absorption spectra (Lambda 950, PerkinElmer) were obtained from diluted SWCNT suspensions in a 1 cm path length quartz cuvette. Zeta potential measurements (Zetasizer Nano ZS, Malvern) were completed using solutions consisting of 0.05 mL of SWCNT suspension diluted into 0.95 mL water and were repeated 6 times. Raman spectra (XplorRA, Horiba Scientific) were obtained from samples dried on glass slides. SWCNT areas were selected using a 100x objective. Excitation wavelengths of 532 nm was used with power adjusted to approximately 10 mW/cm^2 using neutral density filters. The spectra were collected using a 1800T grating with data accumulated over 60 s and averaged from 3 repetitions. Each sample was measured 5 – 15 times to ensure data represent the whole sample.

Auger Electron Spectroscopy and simultaneous Secondary Electron Microscopy was performed on a PHI710 Scanning Auger Nanoprobe. The vacuum pressure in the analysis chamber during analysis was maintained at approximately 10^{-10} Torr. A 10kV electron beam was used for analysis, with a beam current of 10nA. Spectra are presented as the first derivative of electron emission intensity with respect to kinetic Energy. This is required due to the high secondary electron background present in all Auger spectroscopy data. Atomic compositions are determined from the differentiated spectra using peak height and sensitivity factors determined by the instrument manufacturer.

X-ray photoelectron spectroscopy was completed using a non-monochromatic Mg K_α X-ray source (200 W) incident upon the sample within a UHV chamber with working pressure of approximately $5x10^{-10}$ mbar. Electron spectra were recorded with a hemispherical Phoibos 100 energy analyser from SPECS with survey spectra recorded with a pass energy of 40 eV and high resolution spectra recorded at a pass energy of 10 eV. Atomic composition data were calculated using sensitivity factors for Mg irradiation using CasaXPS software version 2.3.16.

Confocal fluorescence microscopy images were collected using a Leica TCS SP5 Scanning Confocal Microscope using a 63x water immersion objective. A drop of water and coverslip were placed on the samples which were dried onto a glass slide. The bright field data were collected using a transmission objective and xenon light source. Fluorescence data were collected using an Ar laser at 488 nm excitation and the emission was collected from 492-561 nm. Photomultiplier tube (PMT) gains and other settings (except zoom level) were consistent for all measurements.

Results and Discussion

Adsorption of ssDNA

Prior to investigating ssDNA desorption from SWCNTs, ssDNA adsorption was investigated to both confirm adsorption and to determine baseline values for characterising subsequent desorption. $(GT)_{20}$ was chosen as the model ssDNA oligomer because it has been used for the chirality specific separation of SWCNTs and because we have found that longer ssDNA strands yield a higher concentration of SWCNT in suspension after probe sonication and centrifugation (typical optical density x dilution factor 20-30, see Figure S1).[5b] The photographs of the suspension in Figure 1 (a) shows the produced SWCNT suspension was stable (for months) and recorded a zeta potential of -42 mV which is similar to other reports of CNT-DNA suspensions and similar in magnitude to SWCNT suspensions with anionic surfactant sodium deoxycholate (Figure S2).[12] SWCNTs dispersed without ssDNA (or surfactant) do not form a stable suspension and do not record a zeta potential value (Figure 2 (a)). Further evidence for ssDNA adsorption was obtained from Raman Spectroscopy, circular dichroism and 2D photoluminescence mapping where a minor chirality preference was observed (more detail in SI, Figure S1 (b)) and Figure S3). The formation of a well suspended SWCNT solution is evidence of ssDNA adsorption but we continued to investigate with complimentary techniques.

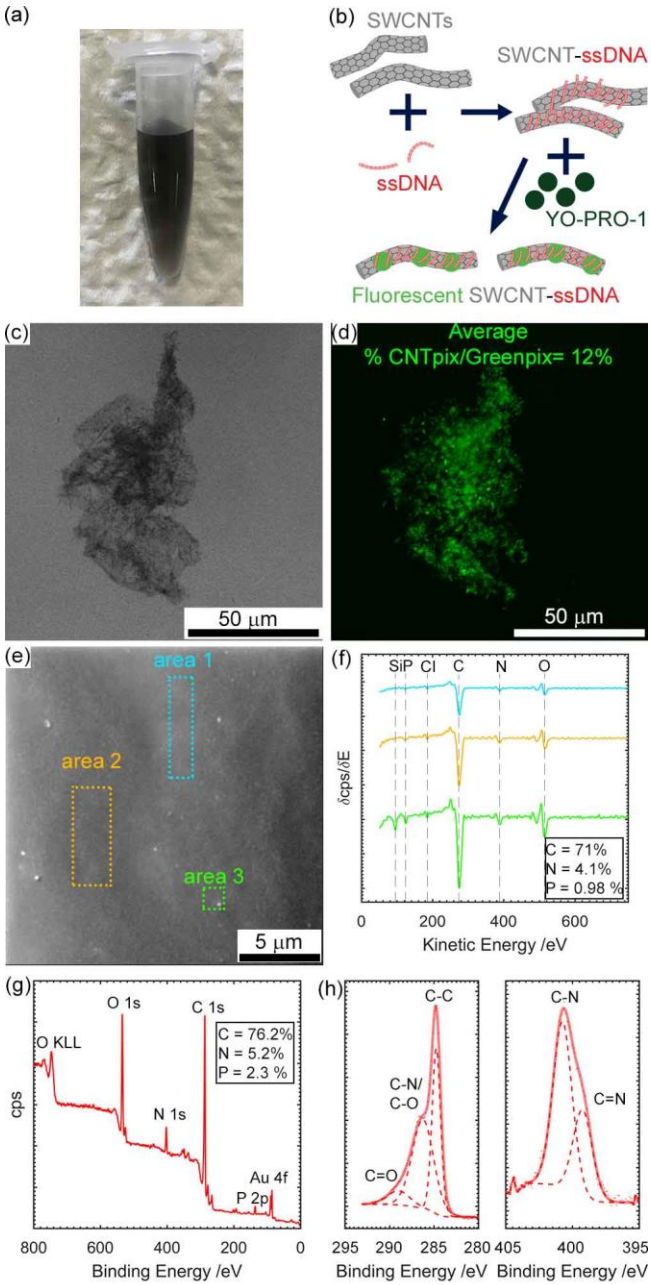

Figure 1: Summary of characterisation of ssDNA adsorption onto SWCNTs and YOPRO1 fluorescence when confined within SWCNT-ssDNA conjugate. (a) Digital photograph of SWCNT-ssDNA suspension. (b) Schematic of ssDNA adsorption onto SWCNT and subsequent fluorescence of YOPRO1 upon intercalation into the conjugate. (c, d) Confocal laser scanning fluorescence microscope of SWCNT-ssDNA-YOPRO1 showing (c) bright field image of dried sample and (d) fluorescence image (ex = 488 nm, em = 510-580 nm) of the same area showing emission from YOPRO1 conjugated within the SWCNT-ssDNA hybrids. (e, f) Scanning Auger microscopy study of SWCNT-ssDNA samples showing (e) SEM image of sample with areas highlighted from which Auger spectra were recorded and presented in (f) along with average atomic percent from multiple samples. (g, f) X-ray photoelectron spectroscopy analysis of SWCNT-ssDNA deposited onto gold coated alumina showing (g) survey spectra with calculated atomic percent and (h) high resolution spectra for C 1s and N 1s with deconvolution.

YOPRO1 is an asymmetric carboncyanine based dye which is known to fluoresce when intercalated within a double stranded DNA helix.[13] Recently YOPRO1 and other similar dyes have been intercalated with SWCNT-ssDNA suspensions to prepare fluorescent hybrids.[14] The constrained environment formed between the ssDNA and SWCNT, like between strands in dsDNA, switches the YOPRO1 from a quenched dark state into a fluorescent state (see schematic in Figure 1 (b)). Confocal fluorescence microscopy images were obtained of the samples after being drop cast onto glass slides

and dried in air at 30 °C. Dried samples were imaged because it allowed for semi-quantitative analysis by comparing the dark areas from the bright field image (Figure 1 (c)), which show white light absorption of the SWCNTs, to the bright green areas from fluorescence from constrained YOPRO1 (Figure 1 (d)). SWCNT-ssDNA-YOPRO1 sample showed fluorescence emission with perfect correlation between SWCNTs and emission. This observation was the same throughout the sample and was reliable and repeatable (Figure S4). Negative control experiments were completed to ensure the YOPRO1 did not fluoresce by itself and did not fluoresce when added to a suspension of SWCNTs without ssDNA (Figure 2 (b-d) and Figure S5).

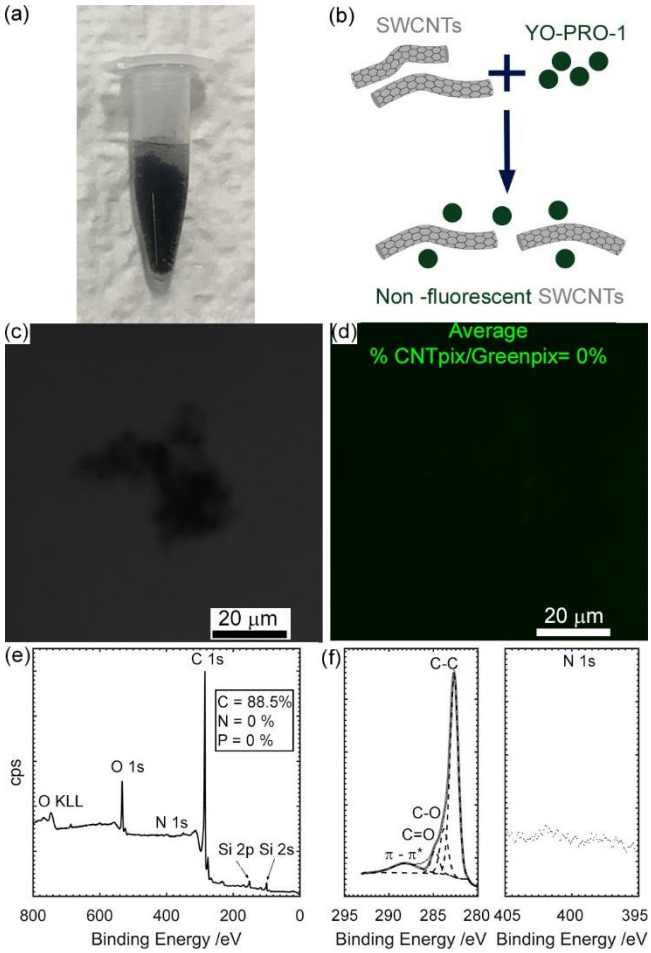

Figure 2: Summary of data for SWCNT (CoMoCAT) suspensions. (a) Digital photograph of 1 mg/mL aqueous suspension. (b) Schematic of SWCNT mixture with YOPRO1 indicating fluorescence of YOPRO1 does not occur when not intercalated. (c, d) Confocal laser scanning fluorescence microscope of SWCNT-YOPRO1 showing (c) bright field image of dried sample and (d) fluorescence image (ex = 488 nm, em = 510-580 nm) of the same area. (e, f) X-ray photoelectron spectroscopy analysis of SWCNT dropcast onto silicon showing (g) survey spectra with calculated atomic percent and (h) high resolution spectra for C 1s and N 1s with deconvolution.

Semi-quantitative analysis of the fluorescence microscope images was completed by counting the number of dark pixels in the bright field image and comparing to the number of green pixels in the fluorescence image. This method and its shortcomings are explained in more detail in the supporting information and Figure S6. SWCNT-ssDNA-YOPRO1 hybrids were found to give a perecentage of fluorescent pixels equal to 12 %. This will serve as a baseline for subsequent desorption experiments.

A third complementary technique that was used to measure ssDNA adsorption was elemental analysis via photoemission spectroscopy. X-ray photoelectron spectroscopy (XPS) and scanning Auger microscopy (SAM) were used to determine the elemental composition of samples either averaged throughout the sample or with spatial resolution. Figure 1 (e, f) depict an SEM image of the SWCNT-ssDNA with Auger emission spectra for the highlighted areas. Quantitative analysis of the obtained spectra give an average atomic % of 71, 4.1, 0.98 % for C, N and P respectively (Figure 1 (e), Table S 1). The N/P ratio is 4.2 which is slightly higher than the N/P ratio of 3.5 for the molecular structure of GT_{20}. Considering there is significant error in quantification of elements with low atomic number and the high secondary electron background in Auger spectroscopy and with low abundance in a sample we consider the discrepancy (4.2 vs 3.5) to be acceptable and will be used for further discussion.

XPS spectra of SWCNT-ssDNA and SWCNT are presented in Figure 1 (h) and Figure 2 (f), respectively. The SWCNT without ssDNA show peaks from C, O and the substrate Si. High resolution XPS are presented in Figure 1 (f) and Figure 2 (d) and show that the carbon 1s peak of the pristine SWCNTs consist of a narrow band at 284.6 eV with smaller contributions from oxidised carbon and a broad π-π* shake up at around 290 eV. In comparison, the C 1s spectra with ssDNA adsorbed onto the CNTs shows that the C1s peak is much broader and can be deconvoluted into several peaks of carbon in various chemical states including C-N and C-O. As expected, nitrogen is not observed for the pristine CNT sample. The survey XPS of SWCNT-ssDNA shows peaks for C, N, P, O in addition to substrate peaks from Au (see Experimental Details). The atomic % calculated is 76, 5.2, 2.3 for C, N and P, respectively. This equates to a N/C ratio of 0.068 which will be used as an approximate quantity of ssDNA for comparison after desorption. The N/P ratio is calculated to be 2.2 which is lower than that for the chemical structure of $(GT)_{20}$ (3.5) but is within a reasonable margin considering the approximations used in the calculation.[15] High resolution N 1s XPS spectra of SWCNT-ssDNA can be deconvoluted into 2 broad peaks that are assigned as various C-N (at 401 eV) and C=N (399.5 eV) groups which are present in the molecular structure of $(GT)_{20}$.[16]

With confirmation of ssDNA adsorption onto the SWCNTs, we then evaluated various procedures for ssDNA desorption with the same (when possible) complementary characterization techniques.

Desorption of ssDNA using biological methods

Exonuclease 1 (exo1) is an enzyme which cleaves nucleotides from ssDNA by breaking phosphodiester bonds from the phosphate backbone.[17] It is regularly used to remove ssDNA in biological systems.[18] SWCNT-ssDNA aqueous suspensions were first centrifuge-filtered using AMICON Ultra 0.5 30K to remove any unbound ssDNA from the solution and to allow solvent exchange to Exonuclease 1 reaction buffer. Exo1 was added and the reaction was allowed to occur for 2.5 – 16 h at RT or 37 ^{o}C. During this period the previously well suspended SWCNT-ssDNA hybrid crashed out of suspension and became a black precipitate at the bottom of the reaction vial. The sample was centrifuge-filtered again to remove enzyme and buffer before being transferred to back into 0.1 M NaCl. The sample could not be resuspended and did not record a zeta potential value (Figure 3 (a)), indicating the electrostatic forces which previously kept the SWCNTs well suspended were no longer present.

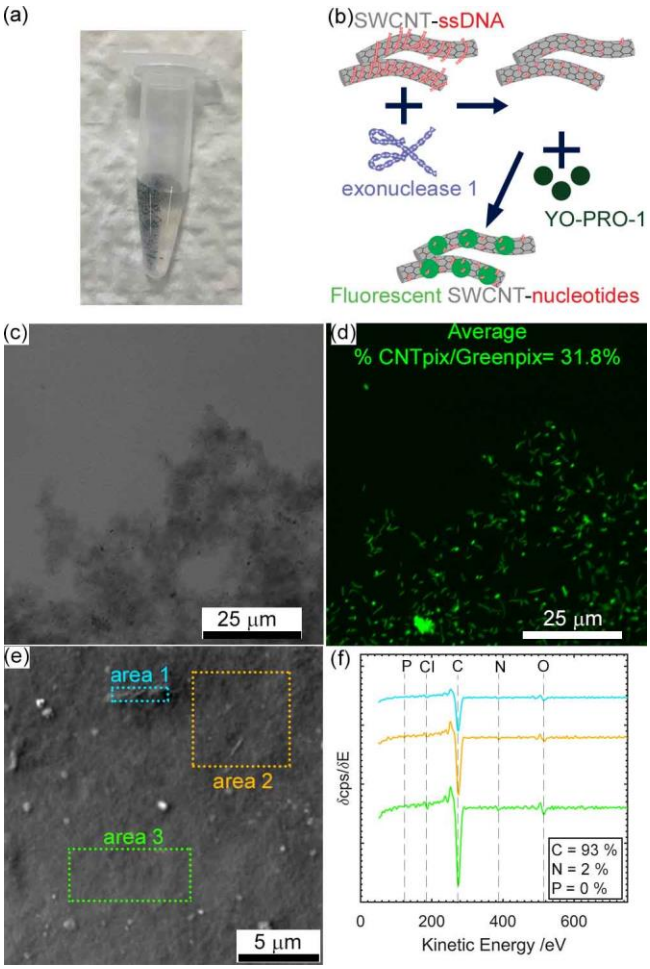

Figure 3: Summary of data for after exo1 treatment of SWCNT-ssDNA dispersion showing (a) digital photograph of the precipitated SWCNT dispersion. (b) Schematic of the process of exo1 cleaving phosphodiester bonds but still allowing YOPRO1 fluorescence. (c, d) Confocal laser scanning fluorescence microscope of SWCNT-ssDNA-exo1-YOPRO1 showing (c) bright field image of dried sample and (d) fluorescence image (ex = 488 nm, em = 510-580 nm) of the same area showing emission from YOPRO1 conjugated within the SWCNT hybrids. (e, f) Scanning Auger microscopy study of SWCNT-ssDNA-exo1 samples showing (e) SEM image of sample with areas highlighted from which Auger spectra were recorded and presented in (f) along with average atomic percent from multiple samples.

The digital photograph of the sample suggests the ssDNA may have been removed by exo1 because a SWCNT precipitate is formed. Precipitation alone has been used in the previous reports to show RNA removal.[10] YOPRO1 was used to probe whether any ssDNA wrapping remained. Representative bright field and fluorescence images are presented in Figure 3 (c, d). It can be seen that the sample is fluorescent in a similar manner to that of SWCNT-ssDNA (Figure 1 b, c) in which the green fluorescence corresponds with the dark areas in the bright field image. Furthermore some features in the fluorescence image have a rod like shape similar to SWCNTs. This result was consistent regardless of time of incubation with exo1 (2.5 – 16 h) or reaction temperature (RT or 37 ^{o}C), see Figure S7). Semi-quantitative analysis completed on 17 separate images gives a %fluorescent pixels of 32 %. This value is significantly higher than that of SWCNT-ssDNA (12 %). We considered whether exo1 adsorbed onto the SWCNTs and then somehow a provided an appropriate environment for YOPRO1 fluorescence. A control experiment of SWCNT only, treated with exo1, then mixed with YOPRO1 was not fluorescent (Figure S8). The discrepancy in values most likely comes from a flaw in the semi-quantitative analysis of these samples in that it does not take into account SWCNT film thickness. It was not possible to reliably deposit thin SWCNT films from the dense precipitated SWCNT sample.

Regardless of the shortcomings of the semi-quantitative analysis, the qualitative observation of strong fluorescence from these samples indicate that ssDNA or nucleotides remain on the SWCNTs. Elemental analysis was completed by SAM where an SEM was used to identify areas of CNTs and then Auger spectra were obtained from the defined areas. The spatial resolution was crucial for the analysis of these samples because only a small amount of material was used for the exo1 treatment and the precipitated SWCNTs could not be transformed into a thin film for XPS analysis. The scanning Auger SEM image and corresponding spectra are shown in Figure 3 (e, f) with all elemental data presented in Table S 2. Auger spectroscopy showed several differences after exo1 treatment compared to SWCNT-ssDNA (Figure 1 (c, d)). Sodium is not observed after exo1 treatment due to the buffer exchange and washing steps involved. Interestingly phosphorus is not observed at all throughout the 29 spectra recorded. The average elemental atomic % was 92.9, 2.1, 0 % for C, N and P respectively.

The complementary characterisation techniques lead us to the following hypothesis. The exo1 cleaves the phosphodiester bonds on the phosphate backbone of the ssDNA adsorbed on the CNTs (Figure 6). The product of this process was that the G and T nucleotides remained adsorbed onto the SWCNT surface while the phosphate backbone was cleaved away. Without the negative charge provided by the phosphate backbone the SWCNTs were no longer able to suspend in water and precipitated. The remaining nucleotides adsorbed onto the SWCNTs are responsible for both the fluorescence of YOPRO1 and presence of N from Auger spectroscopy. The removal of the phosphate backbone is supported by the absence of P from SAM.

Desorption of ssDNA using thermal methods

Thermal desorption is an attractive method to remove various surfactants that are used to disperse SWCNTs. This is because deposition of thin films is simpler for well dispersed (surfactant wrapped) SWCNTs and thermal desorption can be completed after deposition. Nanoelectronic devices from SWCNT-ssDNA mixtures have been prepared by post-deposition oxidative heating in air at 250-300 ^{o}C but little evidence was given to confirm ssDNA desorption.[7] CNTs degrade in oxygen rich atmosphere at around 400 ^{o}C but are stable to much higher temperatures (>1000 ^{o}C) in inert atmosphere or vacuum, as confirmed by thermogravimetric analysis.[19] Here we chose to heat the SWCNT-ssDNA sample in ultrahigh vacuum (~1 x 10^{-9} mbar) up to 400 ^{o}C and monitor ssDNA desorption *in situ* with XPS.

Figure 4 (a) is an XPS spectrum of SWCNT-ssDNA after heating to 400 ^{o}C for 110 min under UHV. There is no appreciable change in the C:N ratio between RT and 400 ^{o}C. Heating time also seems to have little effect on the C:N ratio (Table S 3). This temperature is beyond that required to remove adventitious carbon from samples prior to UHV analysis. To further investigate ssDNA was dropcast onto Si and heated to 400 ^{o}C with XPS measurements completed every 100 ^{o}C (Summary of data in Table S 4). The C:N ratio decreases with temperature indicating desorption of ssDNA from the substrate. However, P increases relative to both C and N with temperature. This indicates that the ssDNA is breaking down and carbon and nitrogen containing species (such as the nueclotides or fractions of the nucleotides) are desorbing from the substrate while phosphorus containing species remain adsorbed. In the case of the ssDNA adsorbed onto the SWCNTs the N:P ratio remains constant while the amount of N increases relative to C. This indicates that the ssDNA remains adsorbed and the carbon lost was probably amorphous or adventitious carbon. The strong adsorption of ssDNA to SWCNTs is supported by various theoretical studies and its strong adsorption to other substrates.[4c, 20]

Our findings from heating both SWCNT-ssDNA and pure ssDNA indicate that heating in inert atmosphere is not an effective method to remove ssDNA.

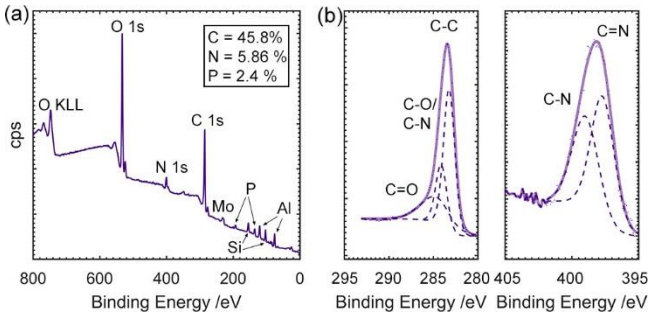

Figure 4: XPS spectra of SWCNT-ssDNA sample deposited onto gold coated alumina after heating to 400 ^{o}C for 110 min showing (a) survey and (b) high resolution scans.

Desorption of ssDNA using chemical methods

Various protocols in literature use chemical methods to remove DNA such as oxidation with H_2O_2,[21] denaturation by changing pH, or by adding organic solvents.[22] In the case of ssDNA, when compared to dsDNA, hydrogen bonding is of less importance but is reported to still play a significant role in adsorption to SWCNTs.[5a, 23] In the following results we compare various chemical treatments including acid, base, oxidiser and salt in their ability to desorb ssDNA.

The specific solutions to desorb the ssDNA from SWCNTs were: 1 M HCl (approx. pH = 1), 1 M NaOH (approx. pH = 14), 50 mM H_2O_2 and 1 M $MgCl_2$. Digital photographs and confocal fluorescence microscopy data are presented in Figure 5 for SWCNT-ssDNA samples treated with the chemical agent for 2 h in a water bath at 60 ^{o}C. The photographs show that all chemical agents caused precipitation of the SWCNT conjugates while the control SWCNT-ssDNA remained well suspended. To determine if ssDNA remained adsorbed after treatment, the samples were washed to remove the chemical agent and YOPRO1 was added. Confocal fluorescence microscopy results indicate that HCl, NaOH and H_2O_2 are effective at desorbing ssDNA while $MgCl_2$ precipitates the suspension but does not desorb ssDNA. The presented fluorescence data were obtained with identical settings to that of the control samples and consequently the dim fluorescence in some samples is difficult to see. The histograms beneath the fluorescence images indicate the quantity of pixels with corresponding colour (x-axis) and can be used to further assess ssDNA removal efficiency.

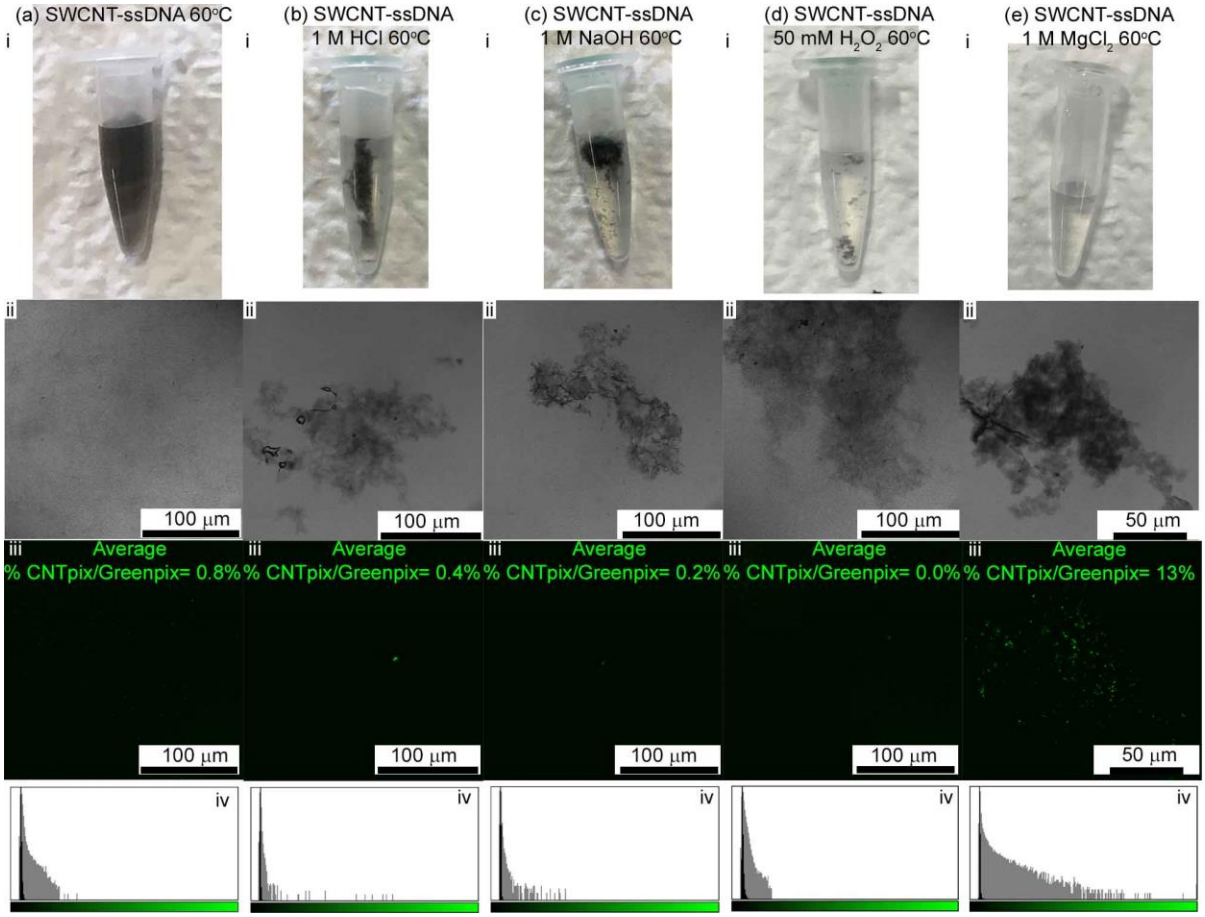

Figure 5: Chemical agents to desorb ssDNA from SWCNTs for 2 h at 60 °C showing (i) digital photograph, (ii) transmission microscope image, (iii) fluorescence microscopy of YOPRO1 (em = 488 nm, ex = 510-580nm) and (iv) colour intensity histogram for the fluorescence image showing normalized counts (black) and log(normalised counts) (grey). The chemical agents shown are (a) heated only, (b) 1 M HCl, (c) 1M NaOH, (d), 50 mM H_2O_2, (e) 1 M $MgCl_2$.

Previous studies using optical characterisation have shown that SWCNT-ssDNA (20 or 21mer ssDNA) conjugates are stable up to 90 °C.[24] The high thermal stability of the conjugates supports the results obtained for in situ heating up to 400 °C under UHV in Figure 4. The YOPRO1 fluorescence intensity of the SWCNT-ssDNA-60°C is observably less than for the sample without heating (Figure 1). This may indicate that there is a morphological change which increases the SWCNT – ssDNA spatial separation which would reduce the fluorescence intensity of YOPRO1. This hypothesis is supported by studies showing an increase in the diameter of gyration of 10mer ssDNA in aqueous suspension with heating to 80 °C.[25] To better show the YOPRO1 fluorescence, the data from Figure 5 are altered in Figure S9 with contrast/brightness optimised. Green rod-like features are observed indicating the SWCNTs remain adsorbed with ssDNA. Thus, the stable suspension and observation of YOPRO1 fluorescence show the ssDNA remains adsorbed with heating to 60 °C.

There are many reactions capable of causing the desorption of ssDNA from SWCNTs observed for the HCl and NaOH treated samples. Desorption will occur if ssDNA is either (1) more stable in a different environment or (2) chemically altered into a form which no longer favours interaction with the SWCNT. Both of these will be discussed in detail.

$(GT)_{20}$ was the ssDNA used in this study. Guanine can exist in several tautomers depending upon the pH of the solution with pKa of ~3.3 for its cationic form and pKa of ~9.5 for its anionic form while

thymine has a pKa of ~9.9 for its anionic tautomer(Figure S10).[26] The acidic and alkaline environments studied were beyond the pKa values for the nucleotide tautomerisation. The ionic base pairs would have a significantly stronger ion – dipole interaction with the solvent than the π-π interactions with the SWCNTs.[27] It is also possible that the change in pH allows for non-Watson-Crick base pairing which has been reported in G rich oligomers (G-G) and for G-T.[28] Bhattacharya *et al.*[24] and Kim *et al.*[29] have shown reversible precipitation of SWCNTs conjugated with C or A rich ssDNA. Both groups claim that reducing pH below the pKa of the nucleotides allows the formation of new secondary structures due to non-Watson-Crick base pairing. The formation of secondary structures results in SWCNT precipitation. Furthermore, the groups found the SWCNT precipitation to be reversible upon returning to neutral pH. We investigated the reversibility of HCl and NaOH treatment by washing the SWCNT precipitate via centrifuge filtration and attempting to resuspend into 0.1 M NaCl. The SWCNTs remained precipitated indicating the mechanism of the initial precipitation was not reversible and permanent damage had occurred to the ssDNA wrapping.

DNA has limited chemical stability and significant damage via hydrolysis and oxidation occur at high rates under physiological conditions but are counteracted by specific DNA repair processes.[22] In the SWCNT-ssDNA systems investigated no such repair processes occur therefore it is likely that significant damage to the ssDNA structure has occured. Figure 6 summarises the bonds susceptible to chemical attack and degradation under the conditions investigated. Hydrolysis of the N-glycosyl bond occurs with the rate depending on temperature, pH, ionic strength and secondary structure.[30] The hydrolysis reaction cleaves the nucleobase from the purine or pyridine with depurination (G, A) occurring with ~20x reaction rate. Without a helical structure, hydrolysis of the N-gylcosyl bond occurs 4x faster for ssDNA.[31] Therefore at high or low pH conditions $(GT)_{20}$ is susceptible to hydrolysis of the N-gylcosyl bond which will cleave the nucleobases. The nucleobases will be cationic or anionic (depending on pH and the nucleobase) and will be more thermodynamically favourable for them to desorb from the SWCNT and suspend in solution. This process would result in permanent desorption of the ssDNA, the SWCNT will precipitate and YOPRO1 would not be fluorescent, as was observed for HCl and NaOH treatment. Considering the evidence we believe hydrolytic attack and ssDNA degradation is responsible for ssDNA removal by HCl and NaOH.

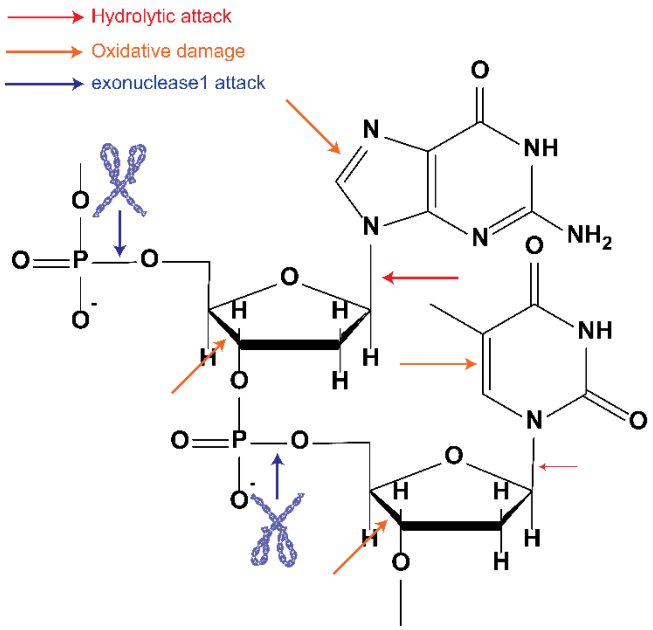

Figure 6: Chemical processes occurring during the desorption of ssDNA, (GT) presented. Red arrows indicate hydrolytic attack which is catalysed under acidic or alkaline conditions with preference for depurination of guanine. Orange arrows indicated bonds susceptible to oxidative damage. Blue arrows shows phosphodiester cleavage by exonuclease1.

HCl and NaOH treatment were also investigated at RT with fluorescence microscopy after YOPRO1 addition presented in Figure S11. The intensity of any fluorescence is very low in comparison to the positive control and similar to that of the samples treated at 60 ^{o}C. Semi quantitative analysis by pixel counting of CNT pixels/YOPRO1 pixels gives 1.8% and 2.8 %. Therefore ssDNA degradation is occurring even at room temperature but a longer time period is required to achieve the same level of ssDNA removal that is reported for elevated temperature.

In addition to pH catalysed hydrolysis, ssDNA is also susceptible to oxidative attack. Oxidation of the deoxyribose moiety can lead directly to strand scission (Figure 6).[32] Guanine and thymine are both susceptible to range of oxidative reactions particularly at double bonds.[33] The resulting modified nucleobases are unstable and are susceptible to further oxidative damage and can become labile. In relevance to the desorption of $(GT)_{20}$ from SWCNT observed for H_2O_2 (Figure 5 (d)) the oxidised ssDNA may either no longer form an attractive non-covalent bond with the SWCNT or the ssDNA may breakdown. The precipitation of the SWCNT suspension was permanent and no YOPRO1 fluorescence was observed.

The precipitation of the SWCNT-ssDNA conjugate with $MgCl_2$ does not result in desorption of ssDNA and YOPRO1 is fluorescent when added to this sample. Divalent Mg^{2+} is commonly used to precipitate DNA samples by reducing the electric double layer and reducing the critical micelle concentration of the suspension.[34] Such attractive interactions of DNA-SWCNT samples have been reported previously to occur in systems where DNA – DNA interactions are repulsive.[35]

Elemental analysis by Auger spectroscopy was obtained for HCl and H2O2 treated samples to ensure complete ssDNA removal. The data are presented in Figure 7 and atomic composition for both samples are presented in Table S 5 and Table S 6. From the 16 unique spectra obtained for the sample with HCl treatment, phosphorus was observed in 3 and nitrogen was observed in 1 with total average atomic percentage of 68, 0.1 and 0.1 % for C, N and P respectively. After H_2O_2 treatment N and P were not observed in any of the 8 unique spectra collected. Similar to fluorescence microscopy results with YOPRO1, it is possible that small fractions of ssDNA remain. Nevertheless, the elemental analysis confirms that the chemical agents are effective at removal of the ssDNA from SWCNTs.

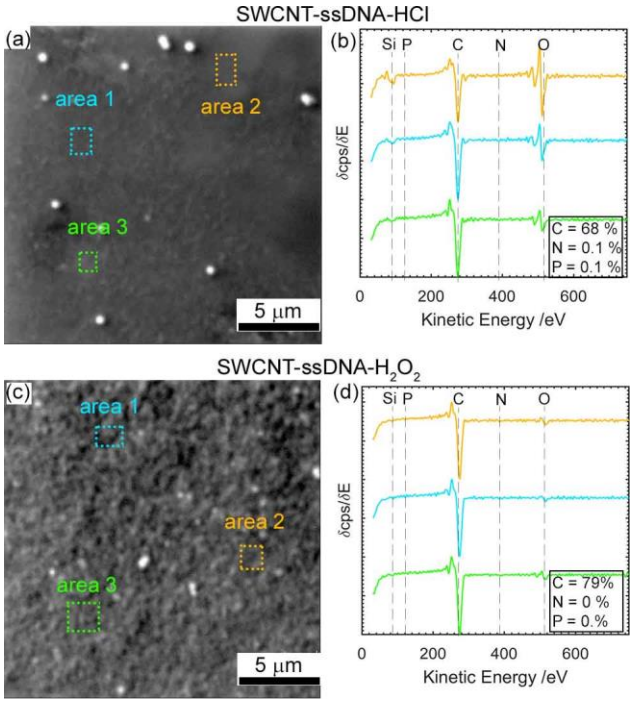

Figure 7: Scanning Auger spectroscopy data of SWCNT-ssDNA samples after chemical treatments showing (a,b) 1 M HCl, 60 °C and (c, d) 50 mM HCl, 60 °C. (a,c) are SEM images with areas highlighted indicating areas from which Auger spectra were obtained in (b, d).

Best practise for ssDNA desorption from SWCNTs

Table 1 summaries the ssDNA desorption methods investigated. The most effective methods to remove ssDNA from SWCNTs was found to be acid, base or oxidising treatment. Higher concentrations and higher temperature of reaction are expected to increase the rate of the reaction but also may lead to SWCNT oxidation. To reduce the likelihood of SWCNT oxidation the reaction can be completed under milder conditions (just above/below pKa of nucleobases) for longer periods.

Considering the complexity of the SWCNT-ssDNA system, a series of complementary techniques should be used to confirm ssDNA desorption. YOPRO1 fluorescence, optical studies such as Raman spectroscopy, and photoemission spectroscopy to determine elemental composition should be used in conjunction to ensure desorption. SWCNT precipitation does not guarantee ssDNA desorption.

Table 1: Summary of SWCNT the effect and proposed mechanism of desorption methods investigated.

Reagent	SWCNT precipitation	ssDNA desorption	mechanism
exonuclease1	Y	N	phosphodiester cleavage, nucleobases remain adsorbed
60 °C	N	N	decrease in YOPRO1 intensity, may alter SWCNT-ssDNA interaction
1 M HCl	Y	Y	hydrolysis of ssDNA
1 M NaOH	Y	Y	hydrolysis of ssDNA
50 mM H_2O_2	Y	Y	ssDNA oxidation
1 M $MgCl_2$	Y	N	increased ionic strength of solvent
400 °C, UHV	N/A	N	Possible nucleobase removal, increasing relative concentration of Phosphorus

Although ssDNA was not entirely removed, exo1 treatment removes the phosphate sugar backbone of the ssDNA via phosphodiester cleavage leaving SWCNT with adsorbed nuclesides and this hybrid structure may be of interest for further investigation. The nucleoside sites may act as seeding points for further hybridisation of the conjugate.

This report has used $(GT)_{20}$ as the model ssDNA for investigation. The mechanism of ssDNA degradation is expected to be similar for other ssDNA oligomers with some slight modifications since, for example, the pKa of tautomers of adenine and cytosine are different but they are still susceptible to hydrolytic attack, especially the purine adenine, and oxidation. ssRNA would hydrolyse at the phosphodiester bond before the N-glycosyl group under the conditions investigated here but further degradation would occur and ssRNA is expected to desorb in a similar manner to the descriptions used for ssDNA.[22]

Conclusions

Thermal and enzyme treatments have been shown to be unsuccessful in the complete removal of ssDNA from the surface of SWCNTs. Exo1 removes the phosphate backbone only, causing SWCNT precipitation, but nucleosides from the ssDNA remain. ssDNA can be effectively removed from the surface of SWCNTs by using a range of chemical treatments. The advantage of the chemical treatments described is that they are universal and will work for all ssDNA sequences. Precipitation is not an effective measure of whether ssDNA is removed but must be complimented with other techniques such as elemental analysis (with spatial resolution if possible) and/or fluorescence from an appropriate dye.

Acknowledgements

The authors acknowledge the facilities of the Australian Microscopy & Microanalysis Research Facility (AMMRF) at Flinders University (Raman, SEM). This work was performed in part at the South Australian node of the Australian National Fabrication Facility, a company established under the National Collaborative Research Infrastructure Strategy to provide nano and micro-fabrication facilities for Australia's researchers. We wish to thank Nigel Spooner and Jillian Moffat (University of Adelaide) for access to, assistance, and expertise in photoluminescence spectroscopy. We also thank Geyou Ao, Jason Streit and Ming Zheng (NIST) for discussion on model ssDNA-SWCNT system and assistance with circular dicroism. This work was funded in part from the Australian Research Council (DP150101354).

Author Contributions

Unless otherwise specified, CJS carried out the experiments, analysed the data and wrote the manuscript. SWCNT-ssDNA samples were prepared by LY who also completed absorbance measurements. Enzyme experiments were conceived and planned by AVE and completed by RF with CJS. Raman data was collected and analysed by CTG and CJS. AS collected Auger spectroscopy data using equipment maintained by JQ. The project was conceived by JGS and GA who gave support to CJS throughout. All authors read the manuscript and approved submission.

References

[1] a)C. Zhao, K. Qu, Y. Song, C. Xu, J. Ren, X. Qu, *Chemistry – A European Journal* **2010**, *16*, 8147-8154; b)H. Sun, J. Ren, X. Qu, *Acc. Chem. Res.* **2016**, *49*, 461-470; c)L. Yu, C. Shearer, J. Shapter, *Chem. Rev.* **2016**, *116*, 13413-13453; dC. J. Shearer, A. Cherevan, D. Eder, *Adv. Mater.* **2014**, *26*, 2295-2318.

[2] S. M. Bachilo, M. S. Strano, C. Kittrell, R. H. Hauge, R. E. Smalley, R. B. Weisman, *Science* **2002**, *298*, 2361-2366.

[3] a)J. R. Sanchez-Valencia, T. Dienel, O. Groning, I. Shorubalko, A. Mueller, M. Jansen, K. Amsharov, P. Ruffieux, R. Fasel, *Nature* **2014**, *512*, 61-64; b)Y. Yuan, H. E. Karahan, C. Yldrm, L. Wei, O. Birer, S. Zhai, R. Lau, Y. Chen, *Nanoscale* **2016**, *8*, 17705-17713.

[4] a)Y. Yomogida, T. Tanaka, M. Zhang, M. Yudasaka, X. Wei, H. Kataura, *Nat. Comm.* **2016**, *7*, 12056; b)A. Nish, J.-Y. Hwang, J. Doig, R. J. Nicholas, *Nat Nano* **2007**, *2*, 640-646; c)M. Zheng, A. Jagota, E. D. Semke, B. A. Diner, R. S. McLean, S. R. Lustig, R. E. Richardson, N. G. Tassi, *Nat Mater* **2003**, *2*, 338-342.

[5] a)X. Tu, S. Manohar, A. Jagota, M. Zheng, *Nature* **2009**, *460*, 250-253; b)G. Ao, C. Y. Khripin, M. Zheng, *J. Am. Chem. Soc.* **2014**, *136*, 10383-10392; c)G. Ao, M. Zheng, *Current Protocols in Chemical Biology* **2015**, *7*, 43-51.

[6] G. Ao, J. K. Streit, J. A. Fagan, M. Zheng, *J. Am. Chem. Soc.* **2016**, *138*, 16677-16685.

[7] a)L. Zhang, X. Tu, K. Welsher, X. Wang, M. Zheng, H. Dai, *J. Am. Chem. Soc.* **2009**, *131*, 2454-2455; b)L. Zhang, S. Zaric, X. Tu, X. Wang, W. Zhao, H. Dai, *J. Am. Chem. Soc.* **2008**, *130*, 2686-2691.

[8] a)R. Yang, J. Jin, Y. Chen, N. Shao, H. Kang, Z. Xiao, Z. Tang, Y. Wu, Z. Zhu, W. Tan, *J. Am. Chem. Soc.* **2008**, *130*, 8351-8358; b)S. Jung, M. Cha, J. Park, N. Jeong, G. Kim, C. Park, J. Ihm, J. Lee, *J. Am. Chem. Soc.* **2010**, *132*, 10964-10966.

[9] a)S. Iliafar, J. Mittal, D. Vezenov, A. Jagota, *J. Am. Chem. Soc.* **2014**, *136*, 12947-12957; b)D. Roxbury, X. Tu, M. Zheng, A. Jagota, *Langmuir* **2011**, *27*, 8282-8293; c)A. Shankar, J. Mittal, A. Jagota, *Langmuir* **2014**, *30*, 3176-3183.

[10] J. C. G. Jeynes, E. Mendoza, D. C. S. Chow, P. C. P. Watts, J. McFadden, S. R. P. Silva, *Adv. Mater.* **2006**, *18*, 1598-1602.

[11] Y. Wu, J. A. Phillips, H. Liu, R. Yang, W. Tan, *ACS Nano* **2008**, *2*, 2023-2028.

[12] A. Zinchenko, Y. Taki, V. Sergeyev, S. Murata, *Nanomaterials* **2015**, *5*, 270.

[13] A. S. Biebricher, I. Heller, R. F. H. Roijmans, T. P. Hoekstra, E. J. G. Peterman, G. J. L. Wuite, *Nature Communications* **2015**, *6*, 7304.

[14] O. Cavuslar, H. Unal, *RSC Advances* **2015**, *5*, 22380-22389.

[15] J. F. Moulder, W. F. Stickle, P. E. Cobol, K. D. Bomben, *Handbook of X-ray Photoelectron Spectroscopy*, Eden Prairie, USA, **1995**.

[16] J. S. Stevens, S. J. Byard, C. C. Seaton, G. Sadiq, R. J. Davey, S. L. M. Schroeder, *PCCP* **2014**, *16*, 1150-1160.

[17] I. R. Lehman, A. L. Nussbaum, *J. Biol. Chem.* **1964**, *239*, 2628-2636.

[18] P. Szankasi, G. Smith, *Science* **1995**, *267*, 1166-1169.

[19] a)S. Aksel, D. Eder, *J. Mater. Chem.* **2010**, *20*; b)A. S. Cherevan, P. Gebhardt, C. J. Shearer, M. Matsukawa, K. Domen, D. Eder, *Energ Environ Sci* **2014**, *7*, 791-796.

[20] B. Shi, Y. K. Shin, A. A. Hassanali, S. J. Singer, *J. Phys. Chem. B* **2015**, *119*, 11030-11040.

[21] E. Linley, S. P. Denyer, G. McDonnell, C. Simons, J. Y. Maillard, *J. Antimicrob. Chemother.* **2012**, *67*, 1589-1596.

[22] T. Lindahl, *Nature* **1993**, *362*, 709-715.

[23] M. Rajarajeswari, K. Iyakutti, Y. Kawazoe, *J. Mol. Model.* **2011**, *17*, 2773-2780.

[24] B. Maji, S. K. Samanta, S. Bhattacharya, *Nanoscale* **2014**, *6*, 3721-3730.

[25] J. Zhou, S. K. Gregurick, S. Krueger, F. P. Schwarz, *Biophys. J.* **2006**, *90*, 544-551.

[26] V. Verdolino, R. Cammi, B. H. Munk, H. B. Schlegel, *The Journal of Physical Chemistry B* **2008**, *112*, 16860-16873.

[27] T. W. G. Solomons, C. B. Fryhle, *Organic Chemistry*, Wiley, **2004**.

[28] a)T. A. Early, J. Olmsted, D. R. Kearns, A. G. Lezius, *Nucleic Acids Res.* **1978**, *5*, 1955-1970; b)J. Trincao, R. E. Johnson, W. T. Wolfle, C. R. Escalante, S. Prakash, L. Prakash, A. K. Aggarwal, *Nat Struct Mol Biol* **2004**, *11*, 457-462; c)D. Sen, W. Gilbert, *Nature* **1988**, *334*, 364-366.

[29] S. R. Shin, C. K. Lee, S. H. Lee, S. I. Kim, G. M. Spinks, G. G. Wallace, I. So, J.-H. Jeong, T. M. Kang, S. Kim, *Chem. Commun.* **2009**, 1240-1242.

[30] L. A. Loeb, B. D. Preston, *Annual Review of Genetics* **1986**, *20*, 201-230.

[31] T. Lindahl, B. Nyberg, *Biochemistry* **1972**, *11*, 3610-3618.

[32] G. Pratviel, J. Bernadou, B. Meunier, *Angewandte Chemie International Edition in English* **1995**, *34*, 746-769.

[33] C. J. Burrows, J. G. Muller, *Chem. Rev.* **1998**, *98*, 1109-1152.

[34] W. E. Razzell, *J. Biol. Chem.* **1963**, *238*, 3053-3057.

[35] X. Qiu, F. Ke, R. Timsina, C. Y. Khripin, M. Zheng, *The Journal of Physical Chemistry C* **2016**, *120*, 13831-13835.

Graphical Abstract

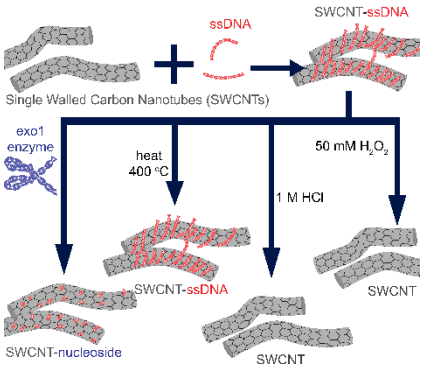

Carbon nanotubes and DNA are commonly hybridised for carbon nanotube purification. Methods are developed to remove single stranded DNA from single walled carbon nanotubes. Enzyme treatment with exonuclease 1 achieves phosphodiester cleavage but nucleosides remain adsorbed. It is found that hydrolytic and oxidative chemical treatments are most promising.